applied sciences

MDPI

Communication

Design of a Compact Indirect Slot-Fed Wideband Patch Array with an Air SIW Cavity for a High Directivity in Missile Seeker Applications

Wootaek Kang [1], Tae-Heung Lim [1,*], Youngwan Kim [2], Sehwan An [2], Ji-Han Joo [2] and Gangil Byun [1]

[1] Department of Electrical Engineering, Ulsan National Institute of Science and Technology (UNIST), Ulsan 44919, Korea
[2] LIG Nex1, Yong-in 16911, Korea
* Correspondence: limth0105@unist.ac.kr

Abstract: This research proposes a compact indirect slot-fed wideband patch array antenna for a missile seeker application. The proposed single antenna consists of three dielectric layers for a radiator, an air substrate-integrated waveguide (SIW) cavity, and an indirect feeding network. The rectangular patch is used as a radiator on the first substrate layer, and the air SIW cavity (ASIWC) is employed to obtain high directivity and low mutual coupling characteristics in the second substrate layer. In the third layer, an indirect feeding structure is used to achieve the wideband characteristics in the Ka-band. The single element is extended to a 4 × 1 linear array with fabrication, and the fabricated array characteristics are measured in a full anechoic chamber. The measured operating fractional frequency bandwidth is 9.2%, and the measured array gain is 11.7 dBi at the bore-sight direction ($\theta_0 = 0^\circ$).

Keywords: cavity-backed antenna; missile seeker; Ka-band; phased array

Citation: Kang, W.; Lim, T.-H.; Kim, Y.; An, S.; Joo, J.-H.; Byun, G. Design of a Compact Indirect Slot-Fed Wideband Patch Array with an Air SIW Cavity for a High Directivity in Missile Seeker Applications. *Appl. Sci.* **2022**, *12*, 9569. https://doi.org/10.3390/app12199569

Academic Editor: Amalia Miliou

Received: 24 August 2022
Accepted: 21 September 2022
Published: 23 September 2022

1. Introduction

With the rapid development of mmWave wireless systems, the use of the mmWave antennas in the Ka-band has been gradually increasing in various civil and military applications, such as 5G communications, healthcare systems, satellite communications, radar systems, and missile seekers [1–8]. In particular, for the military system, recent missile seekers are often required to employ such Ka-band antennas for a low-cost, lightweight, and small antenna size because of a single explosion. The missile seeker antennas are conventionally designed by using 3D structures, such as a Vivaldi type [9,10], a horn type [11,12], a rod type [2,13], and a Yagi–Uda type [14,15], to provide a high directive pattern for precise target tracking. However, these antenna designs have a bulky size and an expensive fabrication cost because their feeding networks commonly need metallic waveguide structures and a sophisticated fabrication process. To overcome the demerits, substantial studies on microstrip patch antennas for a low cost and miniaturization have been investigated by employing various techniques that are the use of a substrate with high-permittivity materials [16,17], a cavity structure [18,19], shorting pins [20,21], and a rectangular ring-shaped patch geometry [22]. Although these techniques can reduce the physical antenna size with a high-directive pattern, those microstrip patch antennas have narrow impedance-matching characteristics because of the direct feeding structure. In addition, when the antennas are extended to an array, the occurrences of the mutual couplings between the adjacent elements degrade the antenna array gain and distort the radiation patterns.

In this paper, we propose a compact cavity-backed wideband patch array using an indirect slot feeding with an air substrate-integrated waveguide (SIW) cavity for a high directivity and a low mutual coupling in the Ka-band. The proposed single antenna is

composed of three dielectric layers for a radiator, an air SIW cavity (ASIWC), and an indirect feeding network. The rectangular patch radiator is printed on a dielectric substrate, and it is co-operated with the ASIWC to achieve a high-directive pattern and a narrow half-power beamwidth (HPBW). An indirect feeding structure is used to obtain the wideband impedance-matching characteristics in the Ka-band. The parametric studies of the proposed single element are conducted, and the essential design parameters of it are then optimized using the HFSS full electromagnetic (EM) simulation software tool [23]. In addition, the mutual coupling characteristics can be enhanced by using the ASIWC when observing the nearfield distributions of a 2 × 1 array antenna. Based on the results, the single element is extended to a 4 × 1 linear array antenna. To verify the antenna performances, the proposed array is fabricated, and its antenna characteristics, such as the reflection coefficients, radiation patterns, and bore-sight gains, are measured in a full anechoic chamber. The result that the proposed array antenna has a high directivity and low mutual couplings is suitable for applying to the missile seeker applications.

2. Design of Proposed Array

2.1. A Stand-Alone Antenna

Figure 1 shows the geometry of a compact stand-alone SIW cavity-backed wideband patch antenna using an indirect slot feeding for a high directivity. The proposed antenna consists of three dielectric layers: a radiator layer (Layer 1), an ASIWC layer (Layer 2), and an indirect feeding network layer (Layer 3).

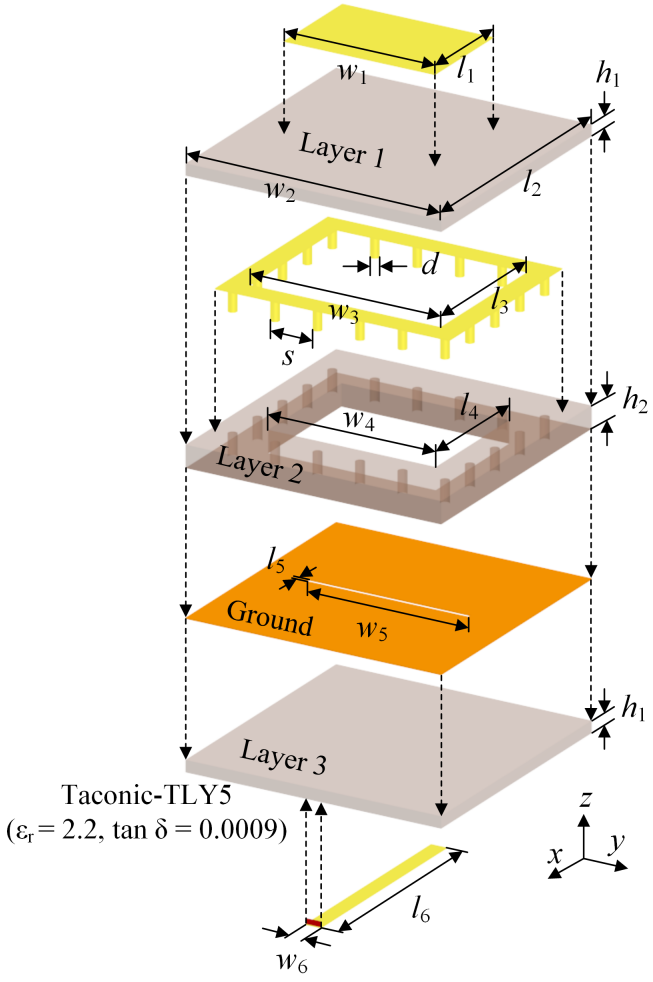

Figure 1. Geometry of the proposed antenna.

On Layer 1, a rectangular patch radiator, having a width w_1 and a length l_1, is printed on a TLY-5 ($\epsilon_r = 2.2$, $\tan\delta = 0.0009$) dielectric substrate ($w_2 \times l_2$) to operate in Ka-band. The patch radiator is driven by the indirect slot feeding network to provide a high-directive radiation pattern with a narrow HPBW. On Layer 2, the ASIWC using the printed patch and vias is designed to substitute a conventional cavity wall [4]. The substrate is perforated in a rectangular shape with dimensions of width × a length × a thickness ($w_3 \times l_3 \times h_2$) to reduce the dielectric loss. In addition, the perforated structure is surrounded by the multiple cylindrical vias with a diameter of d and an interval of s. Then, the vias are electrically connected by a ring-shaped patch printed on the substrate to create the ASIWC-backed structure. The width and length of the ASIWC are w_4 and l_4, and these parameters, including the substrate height h_2, can achieve the high directivity with the narrow HPBW. On the top of Layer 3, a thin rectangular slot ($w_5 \times l_5$) is etched on the ground to indirectly excite the field to the radiator, and the microstrip line ($w_6 \times l_6$) is printed on the bottom of Layer 3 to have a coupled feed for the slot aperture. This indirect feeding network can obtain a wide impedance-matching characteristic in Ka-band compared to the conventional direct feeding technique using a feed pin [24]. It is because two separated resonances of the patch and slot are provided by the proposed feeding network, and the resonances are close to each other for enhancing the matching bandwidth when optimizing the slot and the ASIWC parameters. In addition, the indirect feeding network is essential in Ka-band due to the difficulty in implementing the feed pin, which has an extremely small radius to directly connect the patch radiator and also has a vulnerable structure to an external shock. To optimize the antenna performances, we have conducted parametric studies for the critical geometry parameters, such as h_2, l_4, and w_5. The optimized design parameters are listed in Table 1.

Table 1. Design parameters and their values of the proposed antenna.

Parameters	Values	Parameters	Values
l_1	2.32 mm	l_2	6 mm
l_3	3.5 mm	l_4	2.87 mm
l_5	0.1 mm	l_6	5 mm
l_7	8.9 mm	l_8	2 mm
w_1	3.55 mm	w_2	6 mm
w_3	6 mm	w_4	4.48 mm
w_5	3.8 mm	w_6	0.366 mm
w_7	27.9 mm	w_8	0.366 mm
h_1	0.127 mm	h_2	0.51 mm
d	0.2 mm	s	1 mm
a	6 mm		

In addition, the low thickness of the ASIWC can concentrate strong EM fields in the patch antenna to minimize the fringing field, which can generate the narrow HPBW. In the increment of the ASIWC length, while maintaining the aspect ratio (w_4/l_4 = 1.35), the bore-sight gain continuously increases due to the reduction in the dielectric loss, and this case allows the HPBW to become narrower because of the high-directive properties of the radiation pattern, as shown in Figure 2b. Figure 2c presents the simulated bore-sight gain and the reflection coefficient according to the slot width of the proposed antenna. The gain and the reflection coefficient have an optimal point in the range of w_5 from 2.6 mm to 5 mm. The length of the slot is an important parameter used for the impedance matching of the proposed antenna, which determines the EM coupling strengths between the patch radiator and the ground as well as the radiation characteristic [25].

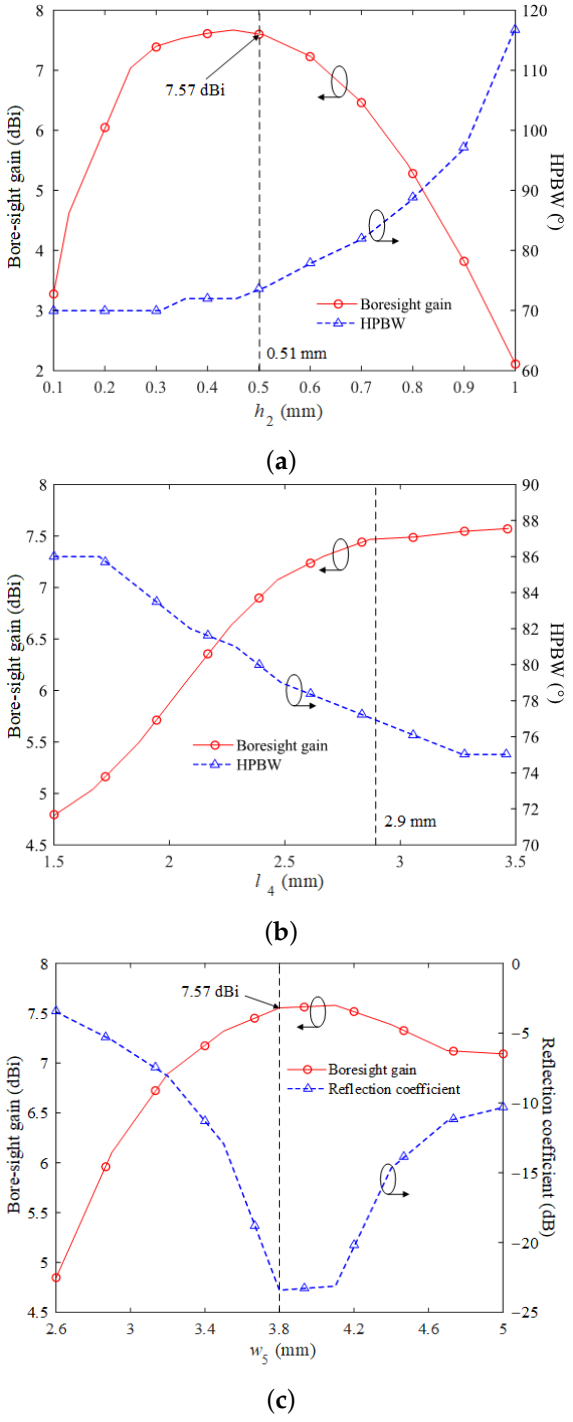

Figure 2. Simulated bore-sight gain, HPBW, and reflection coefficient according to the parameters: (**a**) h_2, (**b**) l_4, and (**c**) w_5.

2.2. An Array Extension

The single element is first extended to 2 × 1 for observing the mutual coupling characteristics when using the ASIWC. Figure 3a,b show the E-field distributions according to the presence and absence of the ASIWC structure. If we draw a specific E-field contour line of 60 dB, the separated E-fields can be observed obviously when employing the ASIWC. Moreover, we simulate S-parameters of the proposed antenna with and without the ASIWC. The mutual coupling value with the ASIWC is decreased by 3 dB less than that without the cavity at the operating frequency of 35 GHz because the multiple vias in the ASIWC can minimize the EM wave propagation from the element to the element through the substrate.

The cavity can additionally miniaturize the antenna size because it can increase the effective permittivity of the substrate [26], that is, the resonant frequency can be changed from 35.9 GHz (without the ASIWC) to 35 GHz (with the ASIWC).

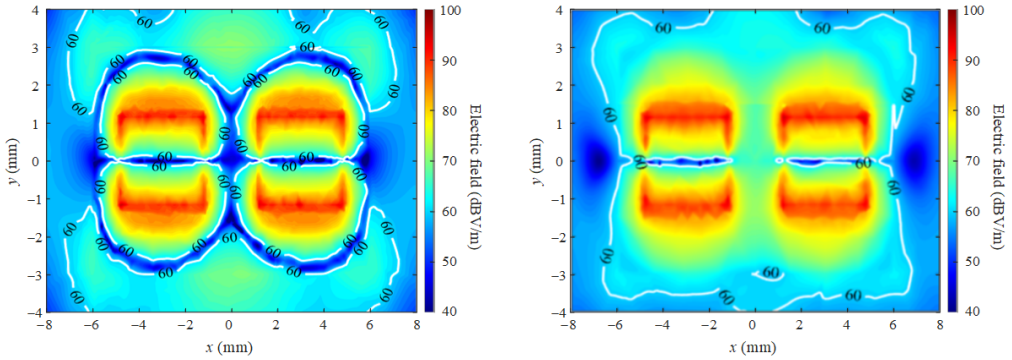

Figure 3. The E-field distributions for the 2 × 1 array antenna: (**a**) with the ASIWC structure, (**b**) without the ASIWC structure.

Figure 4 presents the geometry of the proposed 4 × 1 linear array antenna from the extension of the single element. All elements are printed on the TLY-5 substrate, having a width of w_7 (=27.9 mm) and a length of l_7 (=8.9 mm), and the array distance between the adjacent elements is a of 6 mm. To steer the array beam pattern, the power-dividing feeding network is designed for the steering angles of $\theta_0 = 0°$, 15°, and 30°. The microstrip line stub length l_8 and width w_8 are determined by 2 mm and 0.366 mm for maintaining the wide impedance-matching bandwidth that the single element has. The results confirm that the proposed array antenna using the ASIWC can effectively improve the isolation and reduce the antenna size with the high directivity in Ka-band.

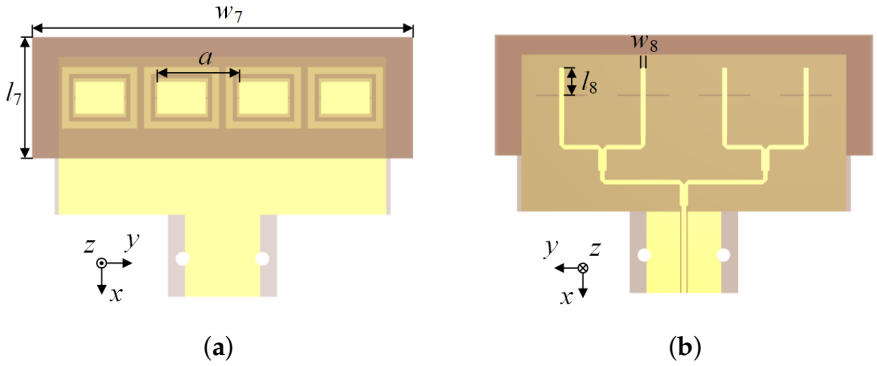

Figure 4. Geometry of the proposed 4 × 1 linear array antenna: (**a**) top view, (**b**) bottom view.

3. Fabrication and Measurement of Proposed Array

Figure 5 illustrates the photographs of the fabricated 4 × 1 linear array antenna using multiple TLY-5 substrate layers. Three different microstrip 4 × 1 power dividers of the feeding network are fabricated to obtain the beam-steering performances at the angles of $\theta_0 = 0°$, 15°, and 30°. For the power excitation, the input microstrip lines of each power divider are connected by employing the end-launch connector (NE03FS001) [27], and each divider has a line loss of 0.8 dB according to the distance (3.77λ at 35 GHz) from the end-launch connector to the slot aperture.

Figure 6 shows the simulated and measured reflection coefficients of the proposed array antenna. The simulation and measurement of the operating fractional frequency bandwidth at 35 GHz are 11.9% and 9.2%, respectively, and those of the reflection coefficient value at 35 GHz are −20.4 dB and −24.08 dB.

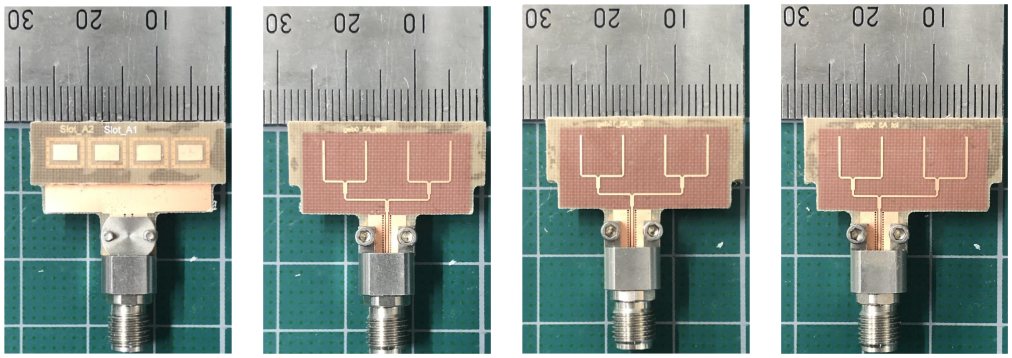

Figure 5. Geometry of the proposed 4 × 1 linear array antenna with power dividers according to the beam-steering angles: (**a**) top view, (**b**) $\theta_0 = 0°$, (**c**) $\theta_0 = 15°$, and (**d**) $\theta_0 = 30°$.

Figure 7 represents the simulations and measurements of 2D radiation patterns according to the steering angles $\theta_0 = 0°$, 15°, and 30° in the *zy*-plane, where the measurements agree well with the simulations. The proposed array has the measured gains of 11.7 dBi ($\theta_0 = 0°$), 10.63 dBi ($\theta_0 = 15°$), and 9.54 dBi ($\theta_0 = 30°$), and the measurements of the HPBW at each steering angle are 16.5°, 19°, and 17°, respectively. Figure 8 presents the measured bore-sight gains in the *zy*-plane at different beam-steering angles according to the frequency compared to the simulations. The measured data at 35 GHz show the bore-sight gains of 11.7 dBi, 10.63 dBi, and 9.54 dBi at the steering angle $\theta_0 = 0°$, 15°, and 30°, and these values are similar to the simulated results of 11.5 dBi, 11.3 dBi, and 9.8 dBi, respectively.

The antenna characteristics, such as the antenna size, a fractional bandwidth, an operating frequency, and so on, of the proposed antenna are compared with those of other previous works [4,5,28,29], as presented in Table 2. The proposed antenna has a higher gain and a narrower HPBW than other works while having a compact size.

Table 2. Design parameters and their values of the proposed antenna.

Ref.	Antenna Size	Fractional Bandwidth (%)	Operation Frequency (GHz)	HPBW (°)	Peak Gain (dBi)	Array Extension
[4]	$0.72\lambda_0 \times 0.72\lambda_0 \times 0.212\lambda_0$	28.5	30	NA	7.34	24 × 24
[5]	$0.41\lambda_0 \times 0.41\lambda_0 \times 0.15\lambda_0$	21.8	27	77	4.9	4 × 1
[28]	$1\lambda_0 \times 1\lambda_0 \times 0.104\lambda_0$	14.7/3.4	28/38	NA	7.5/9.1	2 × 2
[29]	$0.47\lambda_0 \times 0.28\lambda_0 \times 0.04\lambda_0$	15.6	38	97.2	6.5	4 × 4
This work	$0.7\lambda_0 \times 0.7\lambda_0 \times 0.09\lambda_0$	9.2	35	76	7.5	4 × 1

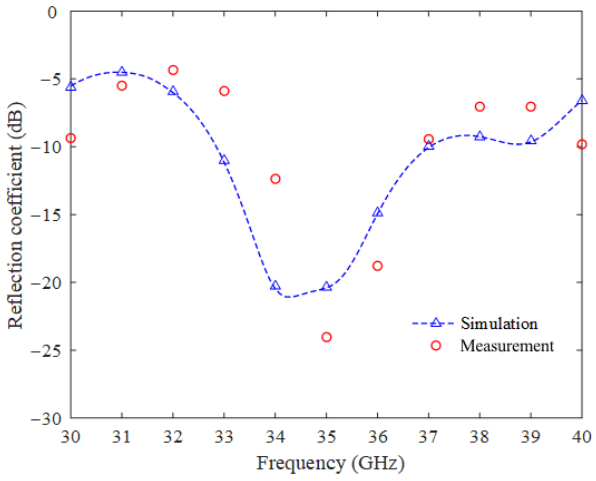

Figure 6. Simulated and measured reflection coefficients of the proposed array antenna.

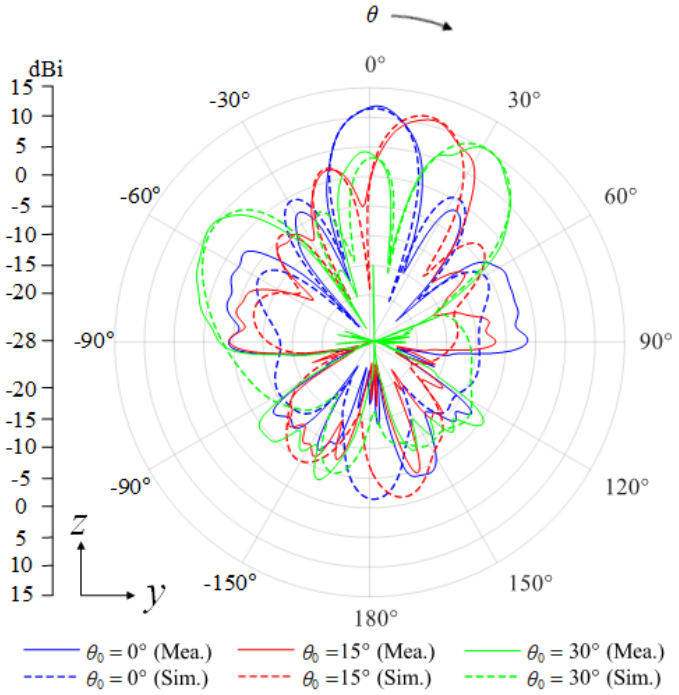

Figure 7. Simulated and measured peak gains at different beam-steering angles.

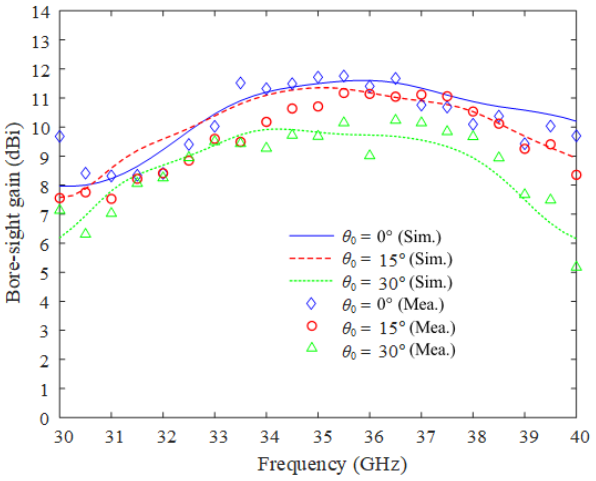

Figure 8. Measured bore-sight gains at different beam-steering angles.

4. Conclusions

We have designed the compact indirect slot-fed wideband patch array using an ASIWC for a high directivity and a low mutual coupling in Ka-band. The rectangular, printed patch radiator was co-operated with the ASIWC to achieve a high-directive pattern, and the indirect feeding structure was used to obtain the wideband impedance-matching characteristics. The 4 × 1 linear array antenna was designed and fabricated to obtain the beam-steering performances. The proposed array obtained the measured gains of 11.7 dBi (θ_0 = 0°), 10.63 dBi (θ_0 = 15°), and 9.54 dBi (θ_0 = 30°) according to the steering angles.

Author Contributions: Conceptualization and methodology, W.K., T.-H.L., G.B., S.A., J.-H.J. and Y.K.; validation and formal analysis, W.K., T.-H.L., G.B., S.A., J.-H.J. and Y.K.; resources and data curation, W.K., T.-H.L., S.A. and J.-H.J.; writing—original draft preparation, W.K.; writing—review and editing, T.-H.L., G.B. and Y.K.; visualization, W.K., G.B. and Y.K.; supervision and project administration, T.-H.L., G.B. and Y.K. All authors have read and agreed to the published version of the manuscript.

Funding: This work was supported by LIG Nex1 Co., Ltd.

Institutional Review Board Statement: Not applicable.

Informed Consent Statement: Not applicable.

Data Availability Statement: Not applicable.

Conflicts of Interest: The authors declare no conflict of interest.

References

1. Bilgic, M.M.; Yegin, K. Wideband Offset Slot-Coupled Patch Antenna Array for X/Ku-Band Multimode Radars. *IEEE Antennas Wirel. Propag. Lett.* **2014**, *13*, 157–160. [CrossRef]
2. Russo, I.; Canestri, C.; Manna, A.; Mazzi, G.; Tafuto, A. Dual-Band Antenna Array With Superdirective Elements for Short-Distance Ballistic Tracking. *IEEE Trans. Antennas Propag.* **2019**, *67*, 232–241. [CrossRef]
3. Hussain, M.; Jarchavi, S.M.R.; Naqvi, S.I.; Gulzar, U.; Khan, S.; Alibakhshikenari, M.; Huynen, I. Design and Fabrication of a Printed Tri-Band Antenna for 5G Applications Operating across Ka-, and V-Band Spectrums. *Electronics* **2021**, *10*, 2674. [CrossRef]
4. Jeong, T.; Yun, J.; Oh, K.; Kim, J.; Woo, D.W.; Hwang, K.C. Shape and Weighting Optimization of a Subarray for an mm-Wave Phased Array Antenna. *Appl. Sci.* **2021**, *11*, 6803. [CrossRef]
5. Tong, X.; Jiang, Z.H.; Yu, C.; Wu, F.; Xu, X.; Hong, W. Low-Profile, Broadband, Dual-Linearly Polarized, and Wide-Angle Millimeter-Wave Antenna Arrays for Ka-Band 5G Applications. *IEEE Antennas Wirel. Propag. Lett.* **2021**, *20*, 2038–2042. [CrossRef]
6. Li, J.; Hu, Y.; Xiang, L.; Kong, W.; Hong, W. Broadband Circularly Polarized Magnetoelectric Dipole Antenna and Array for K-Band and Ka-Band Satellite Communications. *IEEE Trans. Antennas Propag.* **2022**, *70*, 5907–5912. [CrossRef]
7. Patriotis, M.; Ayoub, F.N.; Tawk, Y.; Costantine, J.; Christodoulou, C.G. A Compact Active Ka-Band Filtenna for CubeSats. *IEEE Antennas Wirel. Propag. Lett.* **2021**, *20*, 2095–2099. [CrossRef]
8. Kiani, S.H.; Altaf, A.; Anjum, M.R.; Afridi, S.; Arain, Z.A.; Anwar, S.; Khan, S.; Alibakhshikenari, M.; Lalbakhsh, A.; Khan, M.A.; et al. MIMO Antenna System for Modern 5G Handheld Devices with Healthcare and High Rate Delivery. *Sensors* **2021**, *21*, 7415. [CrossRef]
9. Bhandari, P.; Jian, L. Compact Wideband Array with Side- Lobe Control. In Proceedings of the 2009 IEEE Antennas and Propagation Society International Symposium, Charleston, SC, USA, 1–5 June 2009; pp. 1–4.
10. Kähkönen, H.; Ala-Laurinaho, J.; Viikari, V. Dual-Polarized Ka-Band Vivaldi Antenna Array. *IEEE Trans. Antennas Propag.* **2020**, *68*, 2675–2683. [CrossRef]
11. Saeidi-Manesh, H.; Saeedi, S.; Mirmozafari, M.; Zhang, G.; Sigmarsson, H.H. Design and Fabrication of Orthogonal-Mode Transducer Using 3-D Printing Technology. *IEEE Antennas Wirel. Propag. Lett.* **2018**, *17*, 2013–2016. [CrossRef]
12. He, Y.; Zhao, X.; Zhao, L.; Fan, Z.; Wang, J.K.; Zhang, L.; Ni, C.; Wu, W.J. Design of Broadband Double-Ridge Horn Antenna for Millimeter-Wave Applications. *IEEE Access* **2021**, *9*, 118919–118926. [CrossRef]
13. Abumunshar, A.J.; Sertel, K. 5:1 Bandwidth Dielectric Rod Antenna Using a Novel Feed Structure. *IEEE Trans. Antennas Propag.* **2017**, *65*, 2208–2214. [CrossRef]
14. Smith, L.P.; Howell, J.C.; Lim, S. A Size-Reduced, 15-Element, Planar Yagi Antenna. *IEEE Trans. Antennas Propag.* **2021**, *69*, 2410–2415. [CrossRef]
15. Mantash, M.; Denidni, T.A. CP Antenna Array With Switching-Beam Capability Using Electromagnetic Periodic Structures for 5G Applications. *IEEE Access* **2019**, *7*, 26192–26199. [CrossRef]
16. Byun, G.; Choo, H.; Kim, S. Design of a Small Arc-Shaped Antenna Array with High Isolation for Applications of Controlled Reception Pattern Antennas. *IEEE Trans. Antennas Propag.* **2016**, *64*, 1542–1546 [CrossRef]
17. Qamar, Z.; Naeem, U.; Khan, S.A.; Chongcheawchamnan, M.; Shafique, M.F. Mutual Coupling Reduction for High-Performance Densely Packed Patch Antenna Arrays on Finite Substrate. *IEEE Trans. Antennas Propag.* **2016**, *64*, 1653–1660. [CrossRef]
18. Byun, G.; Hur, J.; Kang, S.; Son, S.B.; Choo, H. Design of a Coupled Feed Structure With Cavity Walls for Extremely Small Anti-Jamming Arrays. *IEEE Access* **2019**, *7*, 17279–17288. [CrossRef]
19. Yun, S.; Kim, D.-Y.; Nam, S. Folded Cavity-Backed Crossed-Slot Antenna. *IEEE Antennas Wirel. Propag. Lett.* **2015**, *14*, 36–39. [CrossRef]
20. Zhang, X.; Zhu, L. Gain-Enhanced Patch Antenna Without Enlarged Size Via Loading of Slot and Shorting Pins. *IEEE Trans. Antennas Propag.* **2017**, *65*, 5702–5709. [CrossRef]
21. Gupta, S.; Mumcu, G. Dual-Band Miniature Coupled Double Loop GPS Antenna Loaded With Lumped Capacitors and Inductive Pins. *IEEE Trans. Antennas Propag.* **2013**, *61*, 2904–2910. [CrossRef]
22. Lim, T.H.; Choo, H.; Byun, G. Design of a Superstrate Module for Simple Resonant Frequency Tuning. *IEEE Access* **2019**, *7*, 43742–43748. [CrossRef]
23. ANSYS HFSS Software. Available online: http://www.ansoft.com/products/hf/hfss/ (accessed on 1 August 2022).
24. Pozar, D.M. Microstrip Antennas. *Proc. IEEE* **1992**, *80*, 79–91. [CrossRef]
25. Chen, C.; McKinzie, W.E.; Alexopoulos, N.G. Stripline-Fed Arbitrarily Shaped Printed-Aperture Antennas. *IEEE Trans. Antennas Propag.* **1997**, *45*, 1186–1198. [CrossRef]

26. Karmakar, N.C. Investigations into a Cavity-Backed Circular-Patch Antenna. *IEEE Trans. Antennas Propag.* **2022**, *50*, 1706–1715. [CrossRef]
27. End Launch Connectors, With-Wave Inc. Available online: https://www.with-wave.com (accessed on 1 August 2022).
28. Hong, T.; Zhao, Z.; Jiang, W.; Xia, S.; Liu, Y.; Gong, S. Dual-Band SIW Cavity-Backed Slot Array Using TM020 and TM120 Modes for 5G Applications. *IEEE Trans. Antennas Propag.* **2019**, *67*, 3490–3495. [CrossRef]
29. Yang, T.Y.; Hong, W.; Zhang, Y. Wideband Millimeter-Wave Substrate Integrated Waveguide Cavity-Backed Rectangular Patch Antenna. *IEEE Antennas Wirel. Propag. Lett.* **2014**, *13*, 205–208. [CrossRef]